J Solid State Electrochem (2007) 11:821–828
DOI 10.1007/s10008-006-0228-6

ORIGINAL PAPER

Preparation and electrochemical behaviors of platinum nanoparticles impregnated on binary carbon supports as catalyst electrodes of direct methanol fuel cells

Seok Kim · Soo-Jin Park

Received: 2 May 2006 / Accepted: 22 September 2006 / Published online: 7 November 2006

Abstract Binary carbon-supported platinum (Pt) nanoparticles were prepared by a chemical reduction method of Pt precursor on two types of carbon materials such as carbon blacks (CBs) and graphite nanofibers (GNFs). Average sizes and loading levels of Pt metal particles were dependent on a mixing ratio of two carbon materials. The highest electroactivity for methanol oxidation was obtained by preparing the binary carbon supports consisting of GNFs and CBs with a weight ratio of 30:70. Furthermore, with an increase of GNFs content from 0% to 30%, a charge-transfer resistance changed from 19 Ohm cm^2 to 11 Ohm cm^2. The change of electroactivity or the resistance of catalyst electrodes was attributed to the changes of specific surface area and morphological changes of carbon-supported catalyst electrodes by controlling the mixing ratio of GNFs and CBs.

Keywords Carbon supports · Platinum nanoparticles · Electrochemical behaviors · Catalyst electrodes · Direct methanol fuel cells

S. Kim
Advanced Material Division,
Korea Research Institute of Chemical Technology,
P.O. Box 107, Yusong,
Daejeon 305-600, South Korea

S.-J. Park (✉)
Department of Chemistry, Inha University,
253, Nam-gu,
Incheon 402-751, South Korea
e-mail: sjpark@inha.ac.kr

Introduction

Direct methanol fuel cells (DMFCs) are attracting much more attention for their potential as clean and mobile power sources in the near future [1–5]. Over the past years, much research was devoted to lowering metallic catalyst loading and electrode overpotential losses. In addition to issues related to metallic electrocatalyst, the structures and properties of carbon supports are also important because they contribute to the overall performance of the electrode [6–13].

On the other hand, the unique properties of graphite nanofibers (GNFs), which are one of the most popular carbon materials have generated an intense interest in the application of these new carbon materials to a number of applications including energy storages, polymer reinforcements, and catalyst supports. Recently, a study is undertaken to explore the physicochemical effects of GNFs-supported metallic particles on the electrocatalytic oxidation of methanol when compared with a traditional supports medium, carbon blacks [9, 10]. Carbon not only conducts electrons and serves as a catalyst support but also helps in the stabilization of the three-phase boundary and morphology of an electrode for fuel cells [11].

The usage of various graphite and carbon black materials as single catalyst support for electrodes was reported. However, with a single carbon support, it may not be easy to control an electrode structure to achieve a combination of high conductivity, high porosity, good morphology, and suitable hydrophobicity. Sakaguchi et al. [12] and Watanabe et al. [13] approached the idea of adopting binary carbon supports for use in liquid electrolyte fuel cells. They have demonstrated the improved utilization of Pt catalyst using this approach.

The main routes for the synthesis of metallic nanoparticle electrocatalysts can be grouped into an impregnation method and a colloidal method. The impregnation method is characterized by a deposition step of Pt or other metal precursors followed by a reduction step. This can be the chemical reduction of the metallic catalysts slurry in solution by using reducing agents (liquid-phase reduction) [11, 14, 15] or gas-phase reduction of the metallic particles impregnated carbon using a flowing H_2 gas stream at a rather high temperature of about 250–600 °C [16, 17]. Compared to this, the colloidal methods [18, 19] have the advantages of producing small and homogeneously distributed carbon-supported metallic nanoparticles, however, the methodologies are very complex.

It is reported that the particle sizes and the loading levels of Pt-based catalysts are key factors that determine their electrochemical activity and cell performance for DMFCs [20–25]. However, the effect of the preparation method and the surface characteristics of various carbon materials have not yet been fully studied to the best of our knowledge.

In this viewpoint, the ideal support material should have the following characteristics: provide a high electrical conductivity, have an adequate water-handling capability at the cathode, and show a good corrosion resistance under oxidizing conditions. While carbon blacks is the common support material for electrocatalysts, new forms of carbon materials such as graphite nanofibers (GNFs) [9, 10] and carbon nanotubes (CNTs) [26–28] were also investigated as catalysts supports. At present, the electrocatalysts are generally supported on high-surface-area carbon blacks with high mesoporous distribution and graphite characteristics. Vulcan XC-72 carbon blacks (Cabot International) is the most commonly used carbon support because of its good compromise between electrical conductivity and specific surface area.

In this paper, we had employed binary carbon supports to fabricate thin film electrodes in DMFCs. The roles of binary carbon supports and optimal mixing ratio will be evaluated and characterized through cyclic voltammetry measurements. It will be shown that with the usage of two carbon supports, electrochemical activities and loading contents of the catalysts can be enhanced. This improvement is further exemplified by the enhanced electrode kinetics of methanol oxidation for a binary carbon support-electrode compared to a single support-electrode.

The objective of this study is to investigate the structural effect of binary carbon supports consisting of GNFs and CBs on the electrochemical properties of the carbon-supported metallic nanoparticles. The sizes and loading levels of metallic nanoparticles were measured by changing the mixing ratio of two types of carbon materials. By changing the mixing ratio of GNFs/CBs, the specific surface area and the morphological structure of the mixed carbon materials are controlled.

Experimental

Materials

The carbon blacks supplied by Korea Carbon Black were used in our experiments. These have an average particle size of 24 nm, DBP adsorption of 153 cc 100 g^{-1} and specific surface area of 112 m^2 g^{-1}. The GNFs were supplied by Showa Denko (Japan). These carbon fiber materials have a diameter of 100–150 nm and a length of 5–50 μm, resulting to a large aspect ratio. They show a rather small specific surface area of 30 m^2 g^{-1}.

Preparation of the carbon-supported Pt nanoparticles

Before the preparation of the Pt-based catalyst, the residual chemicals of the carbon materials used were removed by a Soxhlet extraction by boiling with acetone at 80 °C for 3 h. Two types of carbon materials were washed several times with distilled water and dried in a vacuum oven at 90 °C for 12 h. Binary carbon supports were prepared by mixing CBs and GNFs with different the mixing ratios. The samples were assigned as GNF0, GNF10, GNF30, GNF50, and GNF100 by changing the weight content of the GNFs to 0%, 10%, 30%, 50%, and 100%. In proportion to this change, the weight content of the CBs changed to 100%, 90%, 70%, 50%, and 0%, respectively.

Carbon-supported Pt nanoparticles were prepared by using a modified polyol synthesis method as reported before [26, 27]. Binary carbon materials (500 mg) with a different mixing ratio of CBs and GNFs were suspended and stirred with an ultrasonic treatment for 20 min in ethylene glycol (EG) solution and then a 104 mg hexachloroplatinic acid (H_2PtCl_6) (Pt: 50 mg, Pt weight percent is 10% against the carbon materials) dissolved EG solution was added dropwise slowly to the above solution and stirred mechanically for 4 h. A 1.0 M NaOH dissolved EG solution was added to adjust the pH of the solution to about 11. A formaldehyde (37%, 1.0 ml) aqueous solution was added to the solution to reduce Pt at 85 °C for 1.5 h, and then the solution was heated at 140 °C for 3 h for a complete reduction of Pt. The whole preparation process was conducted under flowing Argon gas. The solid was filtered and washed with 2 L of deionized water and then dried at 70 °C for 24 h.

Characterization of the catalysts

All of the Pt-based carbon catalyst (Pt/C) samples were characterized by recording their X-ray diffraction (XRD) patterns on a Rigaku X-ray diffractometer (Model D/Max-III B) using Cu Kα radiation with a Ni filter. The morphology of the mixed carbon-supported Pt catalysts was observed by

means of a scanning electron microscope (SEM, JEOL JSM-840A SEM). The Pt loading level was calculated by considering the atomic ratio of Pt intensity against carbon intensity by using an energy dispersive X-ray spectroscopy (EDS) method coupled with SEM (JEOL JSM-840A SEM/LINK system AN-10000/85S energy dispersive X-ray spectrometer). Alternatively, the Pt loading level was also measured by using a Jobin-Yvon Ultima-C inductively coupled plasma-atomic emission spectrometer (ICP-AES).

Electrochemical characterization

To check the electroactivity of the catalysts, the cyclic voltammetry method for a three-electrode cell system was performed. We prepared a working electrode by coating the catalyst powder mixed with Nafion® polymer onto a glassy carbon electrode. The preparation of thin film electrodes followed the method described by Schmidt et al. [29]. Glassy carbon electrodes (3 mm in diameter, 7.1 mm^2) served as a substrate for the catalyst materials. Aqueous catalyst suspensions of 20 μg ml^{-1} were dispersed ultrasonically in water and a 200 μl aliqot was transferred onto the glassy carbon substrate, yielding a noble metal loading of ~56.3 μg cm^{-2}. After the evaporation of the water in a nitrogen stream, the resulting thin catalyst film was covered with 80 μl of a 0.1% Nafion® solution to fix the particles on the substrate. The resulting Nafion® film had a thickness of about 0.2 μm. Therefore, it was sufficiently thin so that film diffusion effects were negligible under these conditions [30, 31]. The catalysts were characterized by stationary current–voltage curves at room temperature in a three-electrode cell. An electrolyte solution of 1 M methanol solution in 0.5 M H_2SO_4 was used. Cyclic voltammetry was studied by using a potentiostat/galvanostat of AUTOLAB/PGSTAT30 (Eco Chemie, The Netherlands). A potential had been changed linearly from 300 mV to 1100 mV vs SCE with a scan rate of 20 mV s^{-1}. Electrochemical impedance spectroscopy (EIS) measurements were studied by means of the abovementioned electrochemical device coupled with FRA2 module (Eco Chemie, The Netherlands) in a frequency range of 1 MHz–0.1 Hz. The electrical conductivity of the catalyst electrodes was obtained using Ohm's Law by measuring the resistivity using the four-probe methods (Resistivity Meter (MCP-T600), Mitsubishi Chemical, Japan).

Results and discussion

Particle size and loading level of the catalysts

To assess the effect of the usage of a binary carbon support on the preparation and electrochemical behaviors of carbon-supported Pt nanoparticles, we prepared the mixed carbon supports consisting of CBs and GNFs with different mixing ratios. After Pt incorporation into the carbon materials, the average crystalline sizes of the Pt nanoparticles were obtained by XRD measurements. Figure 1a–e shows the powder X-ray diffraction patterns of Pt catalysts deposited on GNF0, GNF10, GNF30, GNF50, and GNF100. With an increase in GNFs contents, a sharp peak at 2θ=26° and a small peak at 2θ=54° gradually increase. This gradual changes of the peak intensity can be clearly explained by the fact that Pt deposited GNF100 shows a strong peak and Pt deposited on GNF0 shows no peak at this position. This means that GNFs in this study have a crystalline graphitic structure. All samples show the typical Pt crystalline peaks of Pt(111), Pt(200), Pt(220) and Pt(311).

This indicates that the Pt particles prepared on various carbon materials show similar loading levels and similar crystalline structures. From this result, it is found that the Pt nanoparticles were successfully deposited on a mixed binary carbon support regardless of the mixing ratio of CBs and GNFs.

To obtain an average crystalline size of Pt nanoparticles, the detailed Pt (220) peaks in the powder XRD patterns of Pt deposited on various mixed carbon supports are shown in Fig. 2. The average size of the Pt nanoparticles was calculated by using a Scherrer equation [32–34] and shown in Table 1. The detailed Pt (220) peaks are curve-fitted by a mixed Gausiann–Lorentzian method according to Radmilovic et al. [33].

$$L = \frac{K\lambda}{B\cos\theta} \tag{1}$$

where L is the mean size of the Pt particles, K is the Scherrer constant (=0.89), λ=0.154 nm, B is the half-height width of the (220) diffraction line, and θ is the Bragg angle in radian unit.

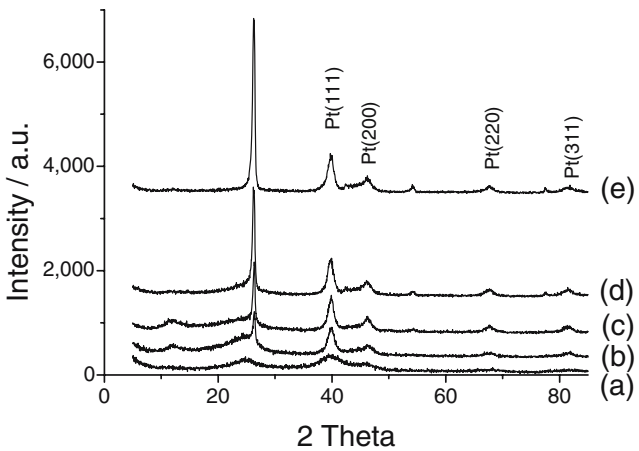

Fig. 1 Powder X-ray diffraction patterns of the Pt catalysts deposited on (**a**) GNF0, (**b**) GNF10, (**c**) GNF30, (**d**) GNF50, and (**e**) GNF100

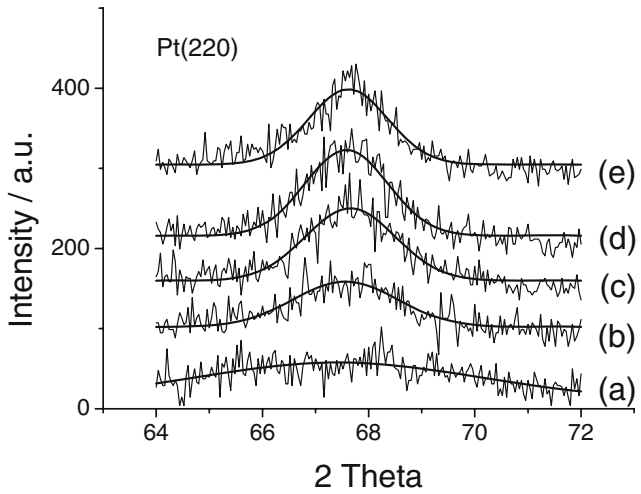

Fig. 2 Detailed Pt (220) peaks in the powder XRD patterns of the Pt catalysts deposited on (**a**) GNF0, (**b**) GNF10, (**c**) GNF30, (**d**) GNF50, and (**e**) GNF100

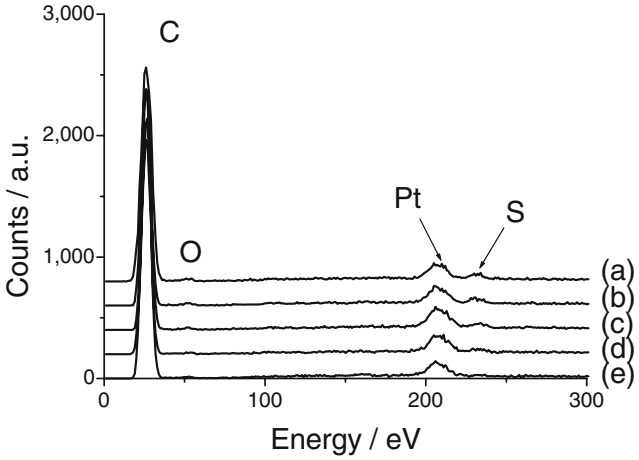

Fig. 3 EDS spectra of the Pt catalysts deposited on (**a**) GNF0, (**b**) GNF10, (**c**) GNF30, (**d**) GNF50, and (**e**) GNF100

The average size of Pt gradually increased from 3.58 to 6.41 nm by changing the GNF content from 0% to 100%. It is interesting to note that a sharpness of peak is enhanced with an increase in GNFs contents. The larger the sharpness of peaks is, the larger the average crystalline size of the Pt particles is. The increase of Pt average size could be related to a decrease of specific surface area by increasing the portion of GNFs, which have smaller specific surface area rather than CBs. This is due to the fact that CBs have a specific surface area of 112 $m^2\ g^{-1}$, while GNFs have a specific surface area of 30 $m^2\ g^{-1}$. Due to the decrease of specific surface area, it is expected that the deposited Pt particles are more aggregated and become larger. From this result, it is concluded that the particle size can be changed by controlling the specific surface area using the mixed carbon supports with different specific surface areas.

Figure 3 shows EDS spectra of the Pt deposited on the mixed carbon supports. The spectra show a strong peak of carbon at 30 eV and a rather small peak of platinum at 210 eV. Platinum loading levels can be calculated by considering the relative peak intensity of Pt against the peak intensity of carbon with an atomic ratio. A 100% loading level of Pt means that the impregnated Pt weight percent is 10% against the carbon materials as described in the "Experimental" section. This value is summarized in Table 2.

In the case of GNF0, the Pt loading level shows a value of 88%. With an increase in GNFs contents up to 30%, the Pt loading level is enhanced to a value of 98%. However, a further increase in GNFs contents over 30% leads to a decrease of the loading level. In the case of GNF100, the Pt loading level shows the smallest value of 73%. This can be explained by the fact that the Pt nanoparticles is not fully impregnated on the carbon surface. Consequently, the Pt loading level shows the highest value of 98%, when the GNFs content is 30%. It is expected that the loading level of Pt deposition can be related to the reaction condition of Pt reduction and surface characteristics of carbon supports. In other words, the loading level is probably dependent on the changes of surface functional groups related with Pt reduction or changes of specific surface area by changing the mixing ratio of two carbon materials. Furthermore, slight peaks of oxygen and sulfur atoms are also shown. Sulfur probably originated from the side product of carbon blacks. From these results, sulfur content is reduced by

Table 1 Average sizes of platinum nanoparticle catalysts deposited on different carbon materials

Carbon samples	Average size (nm)
GNF0	3.58
GNF10	4.87
GNF30	5.62
GNF50	6.13
GNF100	6.41

Table 2 Loading levels of platinum nanoparticles and sulfur contents of 10 wt% Pt/GNF-CB catalysts

Carbon samples	Pt loading level[a] (%)	Pt loading level[b] (%)	Sulfur content[a] (wt%)
GNF0	88	86	1.12
GNF10	93	89	0.99
GNF30	98	95	0.75
GNF50	85	82	0.53
GNF100	73	72	0.02

A 100% loading level means that the impregnated Pt weight percent is 10% against the carbon materials. Sulfur content was referenced to the total weight of the catalysts.

[a] EDS measurements

[b] ICP-AES measurements

increasing the content of GNFs. It is thought that side products such as sulfur can deteriorate the function of the catalysts.

The Pt loading level is also measured independently by using an ICP-AES method. It is also demonstrated in Table 2 for comparison. The values are slightly different from those of the EDS method due to the existence of a little inhomogeneous distribution of Pt nanoparticles in the case of the EDS method. However, the relative value of the Pt loading level between samples shows similar trends.

Electroactivity of the catalysts

Figure 4 shows the electroactivity of the Pt catalyst supported on the mixed carbon supports by cyclic voltammograms. The voltammetric features are consistent with the previous reports [25, 35, 36]. Anodic peaks for a methanol oxidation were shown at 640–740 mV for a forward scan and another anodic peaks were shown at 390–510 mV for a backward scan for each sample. The latter anodic peaks are known to be related to the removal of incompletely oxidized carbonaceous species formed in the forward scan

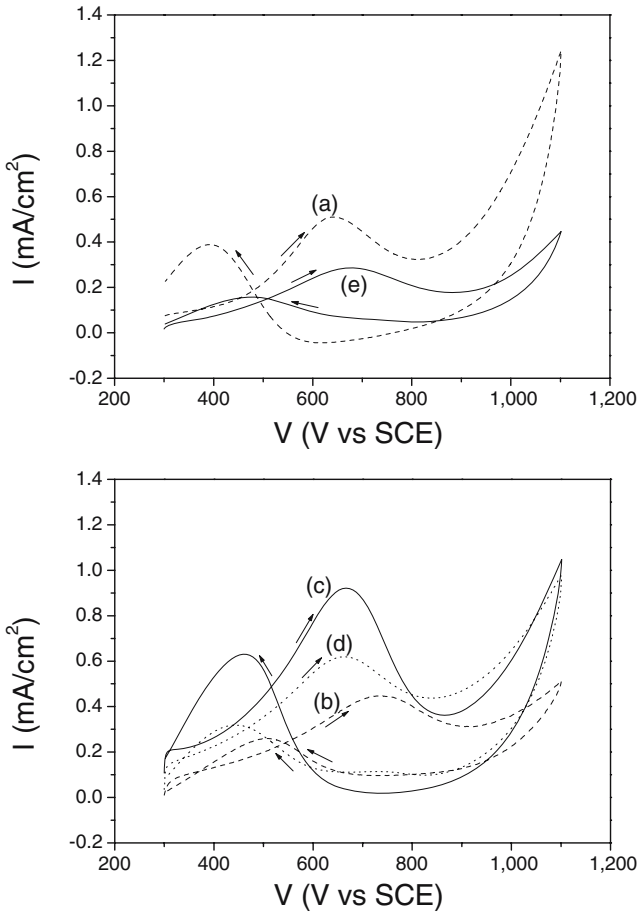

Fig. 4 Cyclic voltammograms of the Pt catalysts deposited on (**a**) GNF0, (**b**) GNF10, (**c**) GNF30, (**d**) GNF50, and (**e**) GNF100, which is measured in 0.5 M H_2SO_4+1.0 M CH_3OH. (Sweep rate: 20 mV s^{-1}, each graph is obtained at the first sweep of multiple sweeps)

[35]. This peak current can be reduced by alloying the Pt catalyst with another metal catalysts for anode catalysts of DMFC [36]. The peak current and potential are described in Table 3. The current density of the anodic peaks increased from 0.489 to 0.989 mA cm^{-2} by increasing GNF contents up to 30%. However, a further increase in GNFs content to over 30% has brought a decrease of current density and a large positive shift of anodic peak potential from 667 to 734 mV. This means that the electroactivity was decayed when the GNFs content is over 30%. From this result, it can be concluded that the electroactivity are the best when the mixing ratio of GNFs and CBs is 30:70. However, this GNF30 sample shows a rather large current density for backward scan. GNF10 shows a rather small current density for backward scan. Consequently, the loading level of Pt incorporation and electroactivity for MeOH oxidation could be changed by controlling the mixing ratio of binary carbon supports. The enhancement of the loading level or the electroactivity originated from the changes in the specific surface area of carbon and morphological changes of the carbon supports by controlling the mixing ratio of GNFs and CBs.

Morphology of the catalyst electrodes

Figure 5a–d shows the SEM micrographs of the Pt-impregnated carbon supports, which have a different mixing ratio of CBs and GNFs. The diameter of GNFs is in the range of 100–150 nm. These GNFs have a large aspect ratio of >500 and a high electrical conductivity of 0.1 S cm^{-1} due to the well-ordered graphitic structure. Pt nanoparticles are not clearly visible in the SEM micrographs because their average sizes are in nanometer scale. By increasing GNFs contents in the order of 10%, 30%, 50%, and 100%, it is clearly shown that the content of the powder-like carbon black particles becomes smaller. Accordingly, it is clearly known that the specific surface area of the carbon supports becomes smaller. This can be one of the reasons why the average size of the Pt particles

Table 3 Electrochemical peak parameters of the catalysts measured by cyclic voltammetry

Carbon samples	Peak potential[a] (mV)	Peak current[a] (mA cm^{-2})	Peak potential[b] (mV)	Peak current[b] (mA cm^{-2})
GNF0	642	0.489	392	0.388
GNF10	664	0.618	508	0.260
GNF30	667	0.989	461	0.630
GNF50	679	0.449	438	0.320
GNF100	734	0.288	477	0.158

[a] Peak in forward scan
[b] Peak in backward scan

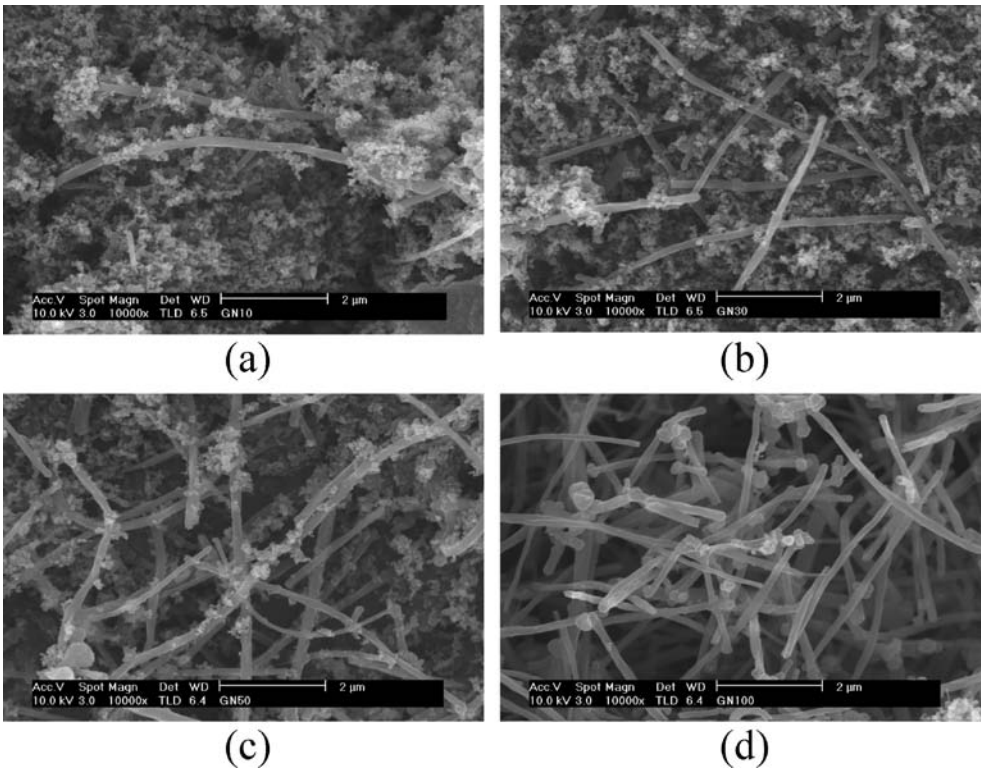

Fig. 5 SEM micrographs of the Pt catalysts deposited on (**a**) GNF10, (**b**) GNF30, (**c**) GNF50, and (**d**) GNF100 (each scale bar means 2 μm in length)

becomes larger. The decrease in specific surface area of the carbon supports can lead to the aggregation of the Pt nanoparticles, resulting to a decrease in effective electrochemical reaction site. However, the volume of vacancy between the carbon particles becomes larger and larger, which can give a free channel of liquid or gas mass transfer. This can function as a beneficial effect on the enhancement of electroactivity. It is thought that the above two adverse effects on the electrochemical activity can explain the existence of an optimum ratio of two different carbon materials.

Impedance and resistance of the catalyst electrodes

Figure 6 shows impedance plots of electrocatalysts in 0.5 M H_2SO_4+1.0 M MeOH. These plots were obtained by measuring AC impedance by changing the frequency from 1 MHz to 0.1 Hz. The plots show a semicircle-like part, though not a perfect shape at a higher frequency range and a linear part at a lower frequency range. When the imaginary part of the impedance value is almost zero, the real part of impedance value indicates the charge-transfer resistance of the catalyst electrode. These resistance values obtained by means of equivalent circuit analysis were demonstrated as a function of GNFs contents in Fig. 7. With an increase in GNFs content from 0% to 30%, the resistance decreases from 19 to 11 Ohm cm^2. With the increase in GNFs content from 30% to 100%, the resistance increases from 11 to 65 Ohm cm^2. These resistance behaviors as a function of GNFs contents show a similar tendency with the above electroactivity results. From this result, the resistance decrease in the case of GNF30 can be one of the reasons for the enhancement of the electroactivity of the Pt catalysts. This change of charge-transfer resistance can be explained primarily by two reasons. The first reason is the difference in the electrical conducting nature of the carbon materials themselves. The other reason

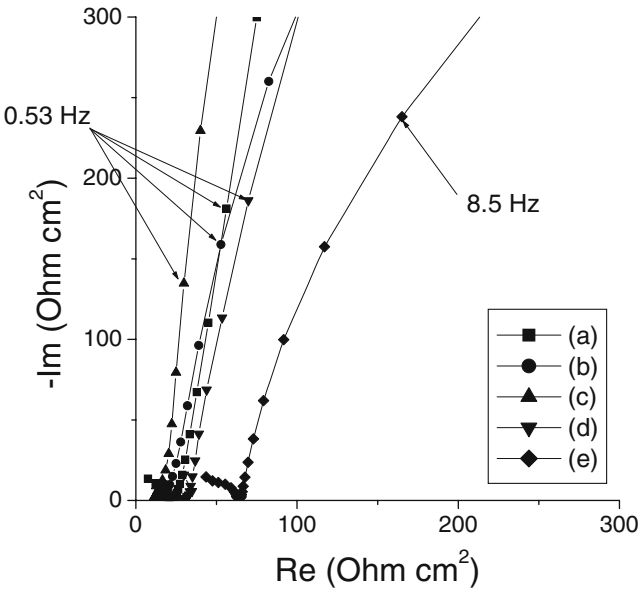

Fig. 6 Impedance plots of the Pt catalysts deposited on (**a**) GNF0, (**b**) GNF10, (**c**) GNF30, (**d**) GNF50, and (**e**) GNF100, which is measured in 0.5 M H_2SO_4+1.0 M CH_3OH

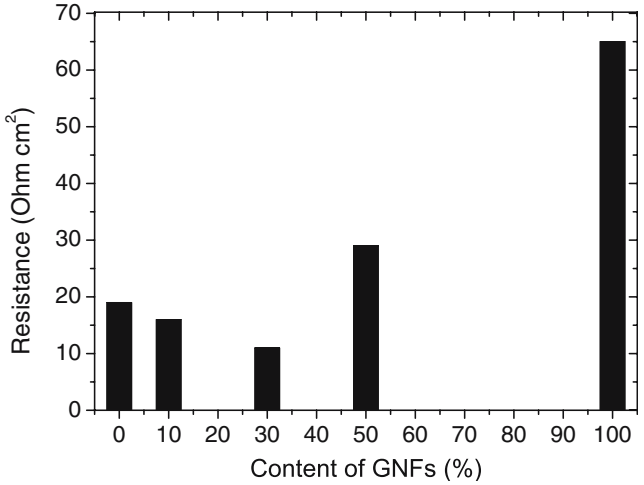

Fig. 7 Resistance changes of the Pt catalysts deposited on (**a**) GNF0, (**b**) GNF10, (**c**) GNF30, (**d**) GNF50, and (**e**) GNF100 obtained from the impedance plots of Fig. 6

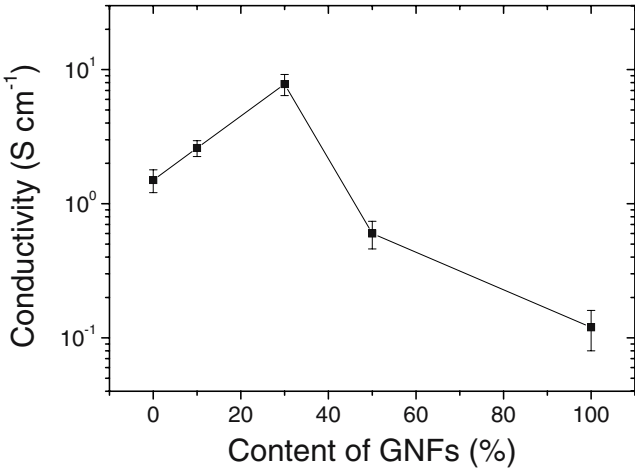

Fig. 8 Electrical conductivity changes of the Pt catalysts deposited on (**a**) GNF0, (**b**) GNF10, (**c**) GNF30, (**d**) GNF50, and (**e**) GNF100

is the change of electrical contact point between the carbon materials, which originated from the morphological change of the Nafion® polymer electrolyte-coated catalyst electrodes.

To check the electrical conduction behaviors of the binary carbon-supported Pt catalyst electrodes, the electrical conductivity was measured by four-probe methods. The samples were prepared by coating Nafion® polymer solution onto Pt deposited on carbon supports. By measuring the electrical conductivity, the electrical conduction could be analyzed between the carbon materials of the catalyst electrode having a polymer electrolyte as an electrically insulating material. Figure 8 shows the electrical conductivity of the catalyst electrodes having binary carbon supports as a function of the contents of GNFs. In the case of GNF0, which uses 100% carbon blacks as carbon supports, the catalyst electrode shows the conductivity of 1.5 S cm^{-1}. By increasing the content of GNFs from 0% to 30%, the conductivity has increased from 1.5 to 7.8 S cm^{-1}. The gradual increase by the addition of GNFs into Nafion®-coated CBs electrodes indicates that the GNFs can function as an electrical conduction bridge between the segregated carbon black aggregates. This can be related to the morphological change of the catalyst electrodes by SEM experiments in Fig. 5. However, when the content of GNFs increases from 30% to 50%, the conductivity has decayed from 7.8 to 0.6 S cm^{-1}. The decrease is probably related to the decrease in electrical contact of carbon black aggregates due to the content decrease of nanoscale powdery carbon blacks. In the case of GNF100, which uses 100% GNFs as carbon supports, the catalyst electrodes show the lowest conductivity of 0.12 S cm^{-1}. Electrical conduction is poor because the electrical contact point is rather insufficient as can be seen in Fig. 5. From this result, the electrical conduction behavior of the catalyst electrodes is strongly dependent on the morphology of carbon-supported catalyst electrodes and this can be one of the origins of the difference in electroactivity of Pt catalyst electrodes.

Conclusions

By using two types of carbon supports such as CBs and GNFs with different mixing ratios, binary carbon-supported Pt catalysts were prepared. The average size of Pt increased from 3.58 to 6.41 nm by gradually changing the GNF content from 0% to 100%. The increase of Pt average size could be related to the decrease in specific surface area by increasing the portion of GNFs, which have smaller specific surface area rather than CBs. On the other hand, the Pt loading level showed the highest value of 98% when the GNFs content is 30%. It could be thought that the loading level of Pt deposition is related to the reaction condition of Pt reduction and surface characteristics of carbon supports.

From the electrochemical experiments, the highest electroactivity for MeOH oxidation could be obtained by preparing the mixed binary carbon supports consisting of GNFs and CBs with a ratio of 30:70. The enhancement of electroactivity originated from the changes in specific surface area and morphological structure (e.g. volume of vacancy, shape or distrubution of vacancy) of carbon-supported catalyst electrodes by controlling the mixing ratio of GNFs and CBs. With the increase in GNFs content from 0% to 30%, the resistance changed from 19 to 11 Ohm cm^2. These resistance behaviors as a function of GNFs contents show a similar tendency with the above electroactivity results. These results are also confirmed by the reverse behaviors of electrical conductivity as a function of the mixing ratio. Consequently, the resistance decrease in the case of GNF30 can be one of the reasons for the enhancement of the electroactivity of the Pt catalysts.

References

1. McNicol BD, Rand DAJ, Williams KR (1999) J Power Sources 83:15
2. Wasmus S, Kuver A (1999) J Electroanal Chem 461:14
3. Arico AS, Srinivasan S, Antonucci V (2001) Fuel Cells 1:133
4. Allen RG, Lim C, Yang LX, Scott K, Roy S (2005) J Power Sources 143:142
5. Scott K, Taama WM, Argyropoulos P (1999) J Power Sources 79:43
6. Joo SH, Choi SJ, Oh I, Kwak J, Liu Z, Terasaki O, Ryoo R (2001) Nature 412:169
7. Kuk ST, Wieckowski A (2005) J Power Sources 141:1
8. Rajesh B, Thampi KR, Bonard JM, Mathieu HJ, Xanthopoulos N, Viswanathan B (2005) J Power Sources 141:35
9. Bessel CA, Laubernds K, Rodriguez NM, Baker RTK (2001) J Phys Chem B 105:1115
10. Steigerwalt ES, Deluga GA, Cliffel DE, Lukehart CM (2001) J Phys Chem B 105:8097
11. Park SJ, Jung HJ, Nah CW (2003) Polymer (Korea) 27:46
12. Sakaguchi M, Uematsu K, Sakata A, Sato Y, Sato M (1989) Electrochim Acta 34:625
13. Watanabe M, Makita K, Usami H, Motoo S (1986) J Electroanal Chem 197:195
14. Liu YC, Qiu XP, Huang YQ, Zhu WT (2002) J Power Sources 111:160
15. Pozio A, Francesco MD, Cemmi A, Cardellini F, Giorgi L (2002) J Power Sources 105:13
16. Cherstiouk OV, Simonov PA, Savinova ER (2003) Electrochim Acta 48:3851
17. Arico AS, Baglio V, Modica E, Di Blasi A, Antonucci V (2004) Electrochem Commun 6:164
18. Bonnemann H, Brinkmann R, Brijoux W, Dinjus E, Joussen T, Korall B (1991) Angew Chem Int Ed Engl 30:1312
19. Gotz M, Wendt H (1998) Electrochim Acta 43:3637
20. Hamnett A (1997) Catal Today 38:445
21. Tang H, Chen JH, Huang ZP, Wang DZ, Ren ZF, Nie LH, Kuang YF, Yao SZ (2004) Carbon 42:191
22. Liu Z, Lin X, Lee JY, Zhang W, Han M, Gan LM (2002) Langmuir 18:4054
23. Liu Z, Lee JY, Chen W, Han M, Gan LM (2004) Langmuir 20:181
24. Jusys Z, Kaiser J, Behm RJ (2003) Langmuir 19:6759
25. Deivaraj TC, Lee JY (2005) J Power Sources 142:43
26. Li W, Liang C, Qiu J, Zhou W, Han H, Wei Z, Sun G, Xin Q (2002) Carbon 40:791
27. Li W, Liang C, Qiu J, Zhou W, Qiu J, Zhou Z, Sun G, Xin Q (2003) J Phys Chem B 107:6292
28. Rajesh B, Ravindranathan TK, Bonard JM, Viswanathan B (2000) J Mater Chem 10:1757
29. Schmidt TJ, Noeske M, Gasteiger HA, Behm RJ (1998) J Electrochem Soc 145:925
30. Watanabe M, Igarashi H, Yosioka K (1995) Electrochim Acta 40:329
31. Schmidt TJ, Gasteiger HA, Stab GD, Urban PM, Kolb DM, Behm RJ (1998) J Electrochem Soc 145:2354
32. Kinoshita K (1988) Carbon: electrochemical and physicochemical properties. Wiley, New York, p 31
33. Radmilovic V, Gasteiger HA, Ross PN (1995) J Catal 154:98
34. Park K, Choi J, Kwon B, Lee S, Sung Y, Ha H, Hong S, Kim H, Wieckowski A (2002) J Phys Chem B 106:1869
35. Liu Z, Ling XY, Su X, Lee JY (2004) J Phys Chem B 108:8234
36. Gao L, Huang H, Korzeniewski C (2004) Electrochim Acta 49:1281